OPEN

HIV-1_{LAI} Nef blocks the development of hematopoietic stem/progenitor cells into T lymphoid cells

Wei Zou[a], Juanjuan Xing[b], Fen Wang[c], Xinping Chen[c], Qian Liu[c], Jinyong Wang[a], Shijie Zou[a], Limin Chen[d], Xin Fu[e], Zhengping Zhou[f] and Zhikai Wan[f]

Objective: Despite successful antiviral therapy, the recovery of $CD4^+$ T cells may not be complete in certain HIV-1-infected individuals. In our previous work with humanized mice infected with CXCR4-tropic HIV-1_{LAI} (LAI), viral protein Nef was found the major factor determining rapid loss of both $CD4^+$ T cells and $CD4^+CD8^+$ thymocytes but its effect on early T-cell development is unknown. The objective of this study is to investigate the influence of LAI Nef on the development of hematopoietic stem/progenitor cells (HSPCs) into T lymphoid cells.

Design: HSPC-OP9-DL1 cell co-culture and humanized mouse model was used to investigate the objective of our study *in vitro* and *in vivo*. RNA-seq was exploited to study the change of gene expression signature after *nef* expression in HSPCs.

Results: *Nef* expression in HSPCs was found to block their development into T lymphoid cells both *in vitro* and in the mice reconstituted with n*ef*-expressing HSPCs derived from human cord blood. More surprisingly, in humanized mice *nef* expression preferentially suppressed the production of $CD4^+$ T cells. This developmental defect was not the result of CD34+ cell loss. RNA-seq analysis revealed that Nef affected the expression of 176 genes in HSPCs, including those involved in tumor necrosis factor, Toll-like receptor, and nucleotide-binding oligomerization domain-like receptor signaling pathways that are important for hematopoietic cell development.

Conclusion: Our results demonstrate that Nef compromises the development of HSPCs into T lymphoid cells, especially $CD4^+$ T cells. This observation suggests that therapeutics targeting Nef may correct HIV-1-associated hematopoietic abnormalities, especially defects in T-cell development.

AIDS 2021, **35**:851–860

Keywords: hematopoietic stem/progenitor cells, humanized mouse model, LAI Nef, RNA-seq, T lymphoid cells

Introduction

HIV-1 infection still poses a serious threat to public health. Its main pathological feature is gradual loss of $CD4^+$ T cells in infected individuals. Although HIV replication and chronic immune activation are thought to cause $CD4^+$ T-cell death, persistent damage to the lymphopoietic system or exhaustion of lymphopoiesis has

[a]Department of Infectious Diseases, [b]Department of Burn, [c]Department of Gynecology and Obstetrics, [d]Center for Experimental Medicine, The First Affiliated Hospital of Nanchang University, [e]Jiangxi Provincial Key Laboratory of Preventive Medicine, School of Public Health, and [f]Department of Clinical Medicine, Nanchang University, Nanchang, Jiangxi, China.

Correspondence to Wei Zou, MD, PhD, Department of Infectious Diseases, The First Affiliated Hospital of Nanchang University, Nanchang 330006, Jiangxi, China.

Tel: +86 15970411802; e-mail: ieeeif@hotmail.com

Received: 11 July 2020; revised: 18 December 2020; accepted: 26 January 2021.

DOI:10.1097/QAD.0000000000002837

been observed in HIV-1-infected individuals [1] suggesting impaired thymic function contributes to $CD4^+$ T-cell loss [2]. In-vitro studies suggest the viral encoded protein Nef and envelope glycoprotein-induced TNFα overexpression be a possible factor mediating HIV-1-induced inhibition of hematopoiesis [3,4]. In addition, HIV-1 may infect CD34+ cells and microvascular endothelial cells and directly disrupt hematopoiesis [5]. These effects of HIV may result in decreased production of naïve $CD4^+$ T cells. It is well known that natural aging leads to thymus degeneration and decreased ability to produce naïve T cells. Studies show HIV infection accelerates aging process [6,7], which compounds thymic degeneration in elderly patients on long-term HIV-1 therapy.

In our previous work Nef was found key in the near elimination of $CD4^+/CD8^+$ thymocytes and $CD4^+$ T cells in the HIV-1_{LAI} (LAI)-infected humanized mice [8,9]. The Nef-dependent loss of $CD4^+CD8^+$ thymocytes may have resulted from direct killing as a result of infection or from indirect effects mediated by extracellular Nef. Recent studies show low levels of hematopoietic stem/progenitor cell (HSPC) infection by HIV-1 may result in functional defect [5,10–12]. However, it is unknown whether Nef is involved in the inhibition of HSPCs by HIV-1. The Nef protein of HIV-1 and simian immunodeficiency virus (SIV) has been shown to inhibit the differentiation of macaque HSPCs into multiple lineages of hematopoietic cells [13]. Thus, the objective of current study is to evaluate the hypothesis that HIV-1 Nef suppresses the development of human HSPCs into T lymphoid cells.

Methods

Isolation of human CD34+ cells

Human CD34+ cells were isolated from umbilical cord blood donated by healthy volunteers at the department of gynecology and obstetrics, The First Affiliated Hospital of Nanchang University. The volunteers were tested negative for HIV, hepatitis B virus, hepatitis C virus, and *Treponema pallidum*. Informed consent was obtained from each volunteer, and the study was approved by the Institutional Ethics Review Board of The First Affiliated Hospital of Nanchang University. Umbilical cord blood mononuclear cells (UCBMCs) were isolated from cord blood on a Ficoll-Paque Plus density gradient (GE Healthcare, Chicago, Illinois, USA). The isolated UCBMCs were then subjected to magnetic separation to isolate CD34+ cells (Miltenyi Biotec, Bergisch Gladbach, Germany; Cat. No.: 130-046-702).

Lentivirus preparation

LAI *nef* (NCBI accession no.: K02013) was cloned into pLVX-EF1a-IRES-Zsgreen1 (Clontech, Mountain View, California, USA) between EcoR I and BamH I sites. Lentiviruses were prepared by transfecting pLVX-EF1a-(NEF)-IRES-Zsgreen1, the packaging vector and VSVG expressing plasmid into 293T cells. Viral particles were harvested and concentrated by Lenti-X Concentrator (Clontech). Viral titer was determined by infecting 293T cells [14].

Lentiviral transduction

CD34+ cells were transduced with the lentiviruses as described previously [15]. A 96-well plate coated with RetroNectin (Clontech) was centrifuged with lentiviruses. Subsequently, the plate was centrifuged with CD34+ cells in StemSpan (Stemcell Technology, Vancouver, Canada) containing stem cell factor (SCF), Flt-3L, IL-6, TPO (R&D, Minneapolis, Minnesota, USA), heparin, monothioglycerol, and polybrene (Sigma, St Louis, Missouri, USA). 72 h after infection, CD34+CD38−ZsGreen1+ cells were sorted with a flow cytometer (Beckman MoFlo XDP; Brea, California, USA).

CD34+ hematopoietic stem/progenitor cell and OP9-DL1 cell co-culture

CD34+ cells were seeded on top of a sub-confluent monolayer of OP9-DL1 cells. The co-culture was performed in α-MEM medium containing fetal calf serum (FCS), streptomycin, penicillin, L-glutamax, IL-7, Flt-3L, and SCF. Every 3–4 days suspension cells were harvested and transferred to a fresh confluent monolayer of OP9-DL1 cells.

Apoptotic assay for lentiviral transduced CD34+ cells

CD34+ cells transduced with LVX-vector or LVX-nef were assessed for apoptosis 48–72 h after transduction by flow cytometry. Annexin V and propidium iodide (BD Pharmingen, San Jose, California, USA) staining was used to differentiate between viable cells and early or late apoptotic cells.

Mice

NCG mice [16,17] were purchased from the Model Animal Research Center of Nanjing University. This mouse model was created by sequential CRISPR/Cas 9 editing of *Prkdc* and *Il2rg* loci in NOD/Nju mice, which carry a mutation in the *Sirpa* gene. Mice were housed in a pathogen-free facility at Jiangxi Academy of Medical Sciences according to Institutional Animal Care and Research Committee-approved protocols. Mice were maintained in individually ventilated cages and fed with sterile food and chlorinated water.

Radiograph irradiation, transplantation, and tissue harvest

NCG mice (6–8 weeks old) were irradiated with 250 rad of radiograph and then transplanted intravenously with $3–5 \times 10^5$ of CD34+ cells transduced with either LVX-vector or LVX-nef. Engraftment and reconstitution of

human cells were assessed every 4 weeks after transplantation for 12 weeks by monitoring the percentage of human CD45+ cells in the peripheral blood. Three months after transplantation, mice were sacrificed, and bone marrow, spleen, and lymph nodes were harvested for the analysis of CD45+, CD3+, $CD4^+$, and $CD8^+$ cells.

Hematoxylin and eosin staining and immunohistochemical analysis

Mouse lymph nodes and spleens were collected, fixed, and embedded in paraffin. Tissue sections were subjected to hematoxylin and eosin (H&E) and immunohistochemistry staining for CD45+, CD3+, $CD8^+$, $CD4^+$, and Nef+ cells with specific antibodies (Abcam, Cambridge, Massachusetts, USA). Photomicrographs were taken with an Olympus camera with 10× and 40× optical objectives (Olympus, Shinjuku, Japan).

Western blotting

Lentiviral transduced CD34+ cells were lysed in RIPA buffer and subjected to SDS–PAGE electrophoresis. Proteins on the membrane were detected with mouse anti-HIV-1 Nef, anti-human β-actin, and goat anti-mouse IgG HRP antibody (Abcam).

Data acquisition and statistical analysis

Immunohistochemistry-positive cells in tissue sections were counted using the NIH Image J software (NIH, Bethesda, Maryland, USA) by three independent individuals with a view field of $100 \times 100\,\mu m$. Cell counting was performed on at least three animals of each group, and three different view fields were chosen randomly in each tissue section. Average values of cell counts were calculated from the pooled data. To ensure objectivity, all sections were blinded for their source and treatments during cell counting. All values were expressed as mean ± SEM. Comparisons between groups were made using two-tailed Student's *t* test in GraphPad Prism version 6 (GraphPad Software, San Diego, California, USA). A *P* value less than 0.05 was considered statistically significant.

RNA-seq and data analysis

Lentiviral transduced CD34+ cells were sorted on the Aria II sorter (BD Biosciences, San Jose, California, USA) to isolate Zsgreen1+CD34+CD38− cells. The cDNA of 500–1000 sorted cells was generated and amplified with the Discover-sc WTA Kit (Vazyme, N711; Nanjing, Jiangsu, China). The quality of amplified cDNA was assessed by quantitative polymerase chain reaction (qPCR) of housekeeping genes (*β2m* and *gapdh*). Samples that passed quality control were used for library construction using the Illumina Nextera XT DNA Sample Preparation Kit (FC-131-1096; Nextra, San Diego, California, USA). All libraries were sequenced with the NextSeq 500 sequencer (Illumina, San Diego, California, USA). The fastq files of raw data were generated using the Illumina bcl2fastq software. Raw read alignment and differential gene expression analysis were performed with software Bowtie2; http://bowtie-bio.sourceforge.net/bowtie2/index.shtml), DESeq2 (https://bioconductor.org/packages/DESeq2/), TopHat2 (http://ccb.jhu.edu/software/tophat/index.shtml), and Cufflinks2.2.1 (http://cole-trapnell-lab.github.io/cufflinks/releases/v2.2.1/) [18,19]. Gene ontology and Kyoto Encyclopedia of Genes and Genomes (KEGG) enrichment analyses (R package ClusterProfiler; http://bioconductor.org/packages/clusterProfiler/) were performed as described previously [20,21]. Protein–protein interaction network analysis was performed with software stringdb (https://string-db.org/). Genes involved in different death pathways were searched in http://amigo.geneontology.org.

Ethics approval and consent to participate

Informed consent was obtained from each volunteer. The current study including all animal experiments (permit no.: 2015-021) was approved by the Institutional Ethics Review Board of The First Affiliated Hospital of Nanchang University. All animal experiments were conducted following the guidelines for housing and care of laboratory animals from the Ministry of Science and Technology of China and in accordance with The First Affiliated Hospital of Nanchang University.

Results

Nef inhibited human T-cell development at the progenitor level

The developmental stages of human T cells from CD34+ HSPCs are illustrated in Supplemental Fig. 1, http://links.lww.com/QAD/C14 [22,23]. To study the effect of Nef on the differentiation of HSPCs to T cells, *nef* gene of LAI was introduced into CD34+ HSPCs by the lentiviral vector LVX-NEF. For controls, another aliquot of human HSPCs from the same donor were transduced with LVX-vector. Each sample from different donors was analyzed separately. The transduction efficiency was 20–30% of all live cells. CD34+CD38−Zsgreen1+ cells were selected by cell sorting and Nef expression in the sorted human HSPCs was confirmed by western blotting with Nef-specific antibody (Fig. 1a). Development of *nef*-expressing human HSPCs into T lymphoid cells *in vitro* was examined by co-culturing them with mouse BM-derived OP9-DL1 cells to promote T-cell differentiation [24,25]. The Nef from CXCR4-tropic LAI was chosen for current study for several reasons. It has been shown X4-tropic viruses are more capable of infecting a broad range of HSPCs and cause hematopoietic abnormalities than R5-tropic viruses in infected individuals [26]. Besides, the peptide 66–97 of LAI Nef inhibits the clonogenicity of CD34+ cells from macaque BM [13].

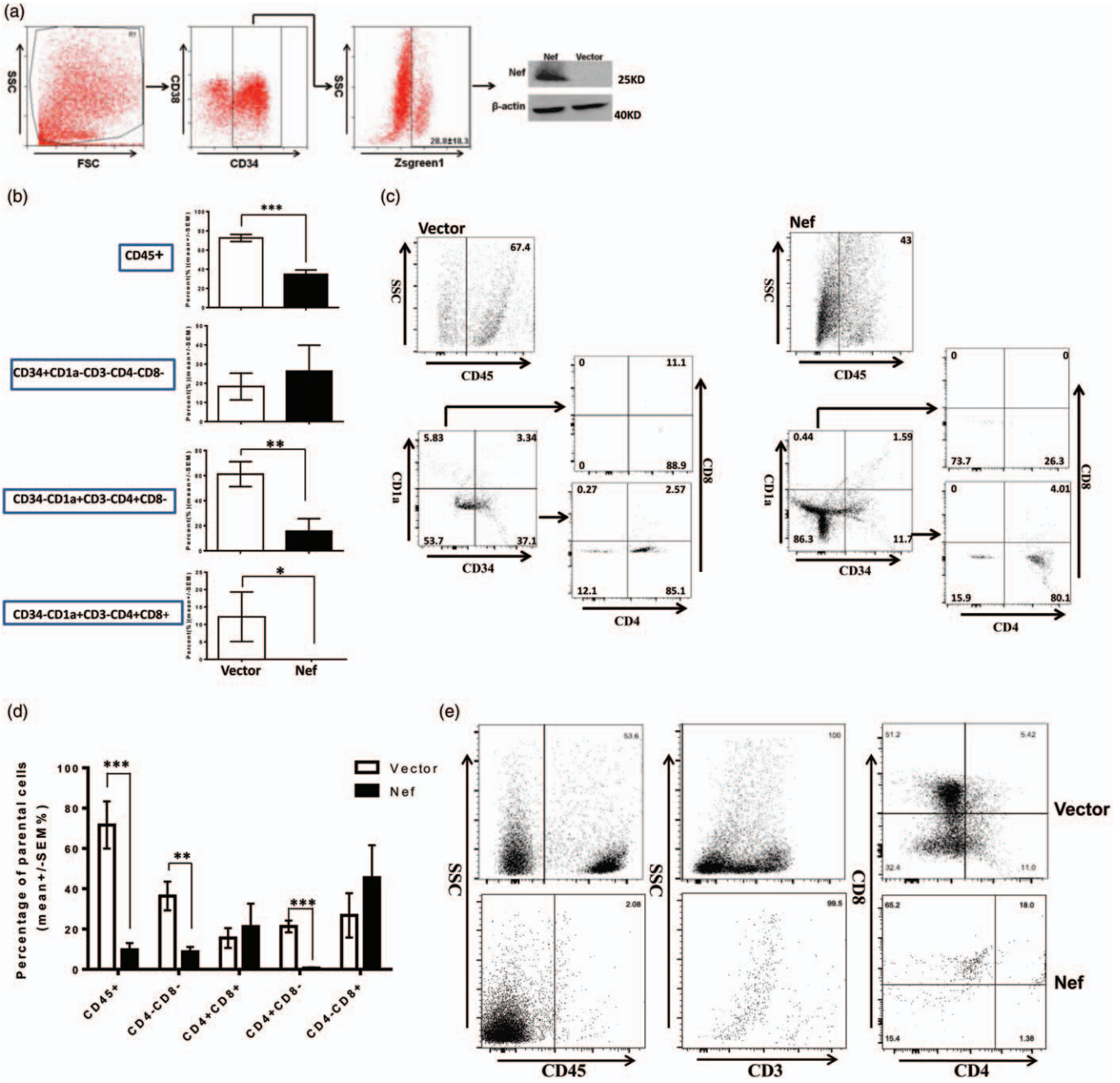

Fig. 1. Effect of Nef on T-cell development in hematopoietic stem/progenitor cell-OP9-DL1 cell co-culture and in the thymus of humanized mice. Expression of Nef protein in flow-sorted CD34+Zsgreen1+ hematopoietic stem/progenitor cells was confirmed by Western blotting with Nef-specific antibody and is shown in (a). Human CD34+ CD38−Zsgreen1+ hematopoietic stem/progenitor cells were seeded in wells of a six-well tissue culture plate with each well containing a sub-confluent monolayer of OP9-DL1 cells. Seven days after co-culture, suspension cells in the culture were collected, and the expression of CD45, CD34, CD1a, CD3, $CD4^+$, and $CD8^+$ on these cells was determined by flow cytometry to differentiate the T cells at different developmental stages. The cumulative flow data are shown in (b) and representative flow data are shown in (c) ($n = 10$ for vector group and $n = 6$ for nef group). 'Percentage' refers to percentage of the parental cell population. The gating strategy was FSC/SSC>CD45>CD34/CD1a>CD3>$CD4^+$/$CD8^+$. To study the effect of Nef on thymocyte development *in vivo*, control or *nef*-expressing CD34+ cells were transplanted into radiograph irradiated immune deficient mice. Three months after transplantation, mice were sacrificed, and thymuses were harvested for isolation of mononuclear cells. These cells were then stained for CD45/CD3/$CD4^+$/$CD8^+$ for flow analysis. Representative flow images are shown in (e), and the cumulative flow data of each type of thymocytes from mice in each group are shown in (d) ($n = 5$ for vector group and $n = 7$ for nef group). $^*P < 0.05$, $^{**}P < 0.01$, $^{***}P < 0.001$.

Seven days after co-culture, suspension cells were harvested and analyzed for surface expression of CD45, CD34, CD1a, CD3, $CD4^+$, and $CD8^+$. Nef expression resulted in a decreased level of CD45+ cells but had no effect on the level of CD34+CD1a−CD3−CD4−CD8− cells relative to the control. However, the levels of CD34−CD1a+CD3−$CD4^+$CD8− and CD34−CD1a+CD3−$CD4^+CD8^+$ cells were significantly decreased in *nef* group compared with the control group and the level of CD34−CD1a+CD3−$CD4^+CD8^+$ cells was lower than that of CD34−CD1a+CD3−$CD4^+$CD8− cells (Fig. 1b and c). This result indicates the differentiation of CD34+ HSPCs to T lymphoid cells was adversely affected by Nef.

To investigate the effect of Nef on the differentiation of HSPCs *in vivo*, radiograph irradiated, immune deficient NCG mice (NOD/Nju$^{Prkdc-/-}$/*Il2rg*$^{-/-}$) were transplanted with sorted, pooled human HSPCs with or without *nef* expression. Pooled HSPCs were used because of insufficient number of cells for transplantation from a single donor. In our model human HSPCs developed into T cells in the mouse thymus. Analysis of the thymocytes from transplanted mice reveal the percentages of CD45+, CD4−CD8−, and $CD4^+$CD8− cells were significantly decreased, but those of $CD4^+CD8^+$ and CD4−$CD8^+$ cells were not changed in the Nef group compared with the control group (Fig. 1d). These results indicate the development of $CD4^+$CD8− cells was more adversely affected by Nef than that of CD4−$CD8^+$ cells. In addition, more cells were present in the thymus of control mice than the Nef group indicating the absolute numbers of $CD4^+CD8^+$ and CD4−$CD8^+$ cells were higher in control mice than the Nef group although the percentages of these two subsets of cells were the same (Fig. 1e).

To determine whether nef expression in CD34+ HSPCs affects cell survival, propidium iodide or annexin V-positive cells were enumerated 48–72 h after transduction. Results indicated the percentage of propidium iodide-positive cells was significantly higher, but that of annexin V-positive nef-expressing CD34+ cells was lower than vector transduced cells (Supplemental Fig. 2, http://links.lww.com/QAD/C15). Further analysis of propidium iodide and annexin V staining of CD34+CD38+ and CD34+CD38− HSPCs revealed CD34+CD38+ cells were more adversely affected by Nef. Taken together, these results suggest more cells in the Nef group were dead than the control group and Nef hindered the production of T lymphoid cells from HSPCs partly by causing their premature death.

Nef decreased the survival of mature T cells

To study the impact of Nef on mature T cells, levels of human T cells in the peripheral blood of the humanized mice transplanted with either vector-expressing or *nef*-expressing HSPCs were monitored every 4 weeks for 12 weeks. Nef expression was found to decrease the levels of CD45+, CD3+, $CD4^+$, and $CD8^+$ cells in the peripheral blood of these mice (Fig. 2a–c). These results were mostly consistent with those found in mouse thymus.

Three months after transplantation, mice were sacrificed, and BM, spleen, and lymph nodes were harvested for flow analysis. Tissue sections of spleens and lymph nodes were analyzed by H&E staining and immunohistochemistry for CD45+, CD3+, $CD4^+$, and $CD8^+$ cells and Nef expression. CD45+ cells in these organs were significantly decreased in the Nef group compared with the control group while $CD4^+$ cells were suppressed in the lymph nodes and spleen but not in the BM. Significantly, $CD8^+$ cells were not suppressed by Nef and in fact appeared to be the dominant T cells in the BM and lymph nodes, especially in the lymph nodes, suggesting Nef may attract more $CD8^+$ cells to lymph nodes. The large drop in $CD4^+$ cells in lymph nodes and spleen may have brought about a decreased level of CD3+ cells in spleen but not in lymph nodes. BM did not exhibit a significant loss of CD3+ T cells even though CD45+ cells were decreased (Fig. 3). In addition, there were more CD4−CD8− cells present in the lymph nodes and spleen when Nef was expressed suggesting these cells could have their cell surface $CD4^+$ down-regulated by Nef, but this effect was not observed in the BM.

H&E staining of the lymph nodes from control mice showed a nearly normal structure in cortex and medulla. Consistent with the flow data, immunohistochemistry (IHC) staining showed abundant CD45+, CD3+, $CD4^+$, and $CD8^+$ cells in the lymph nodes of control mice. Very few and smaller lymph nodes were found in the Nef mice, suggesting Nef adversely affected the development of hematopoietic cells and formation of lymph nodes (Fig. 4a and c). These results are consistent with what has been reported recently that HIV-1 Nef disrupts $CD4^+$ T lymphocyte polarity, extravasation and homing to lymph nodes via the nef-associated kinase complex interface [27].

In the spleens of control mice, white and red pulps were easily recognized with H&E staining, and IHC staining revealed CD45+, CD3+, $CD4^+$, and $CD8^+$ cells were extensively reconstituted (Fig. 4b). However, in the Nef mice, white and red pulps were not distinguishable by H&E staining, and only a limited number of sporadic clusters of CD45+, CD3+, $CD4^+$, and $CD8^+$ cells were detected by IHC staining (Fig. 4b). Quantitative counting of these cells showed the numbers of all of these cells in the spleens of the Nef mice were significantly reduced compared with the control mice (Fig. 4c). These results indicated Nef inhibited the reconstitution of CD45+, CD3+, $CD4^+$, and $CD8^+$ cells in lymphoid organs of humanized mice.

To further confirm the expression of Nef in the humanized mice, spleens from the vector and Nef group

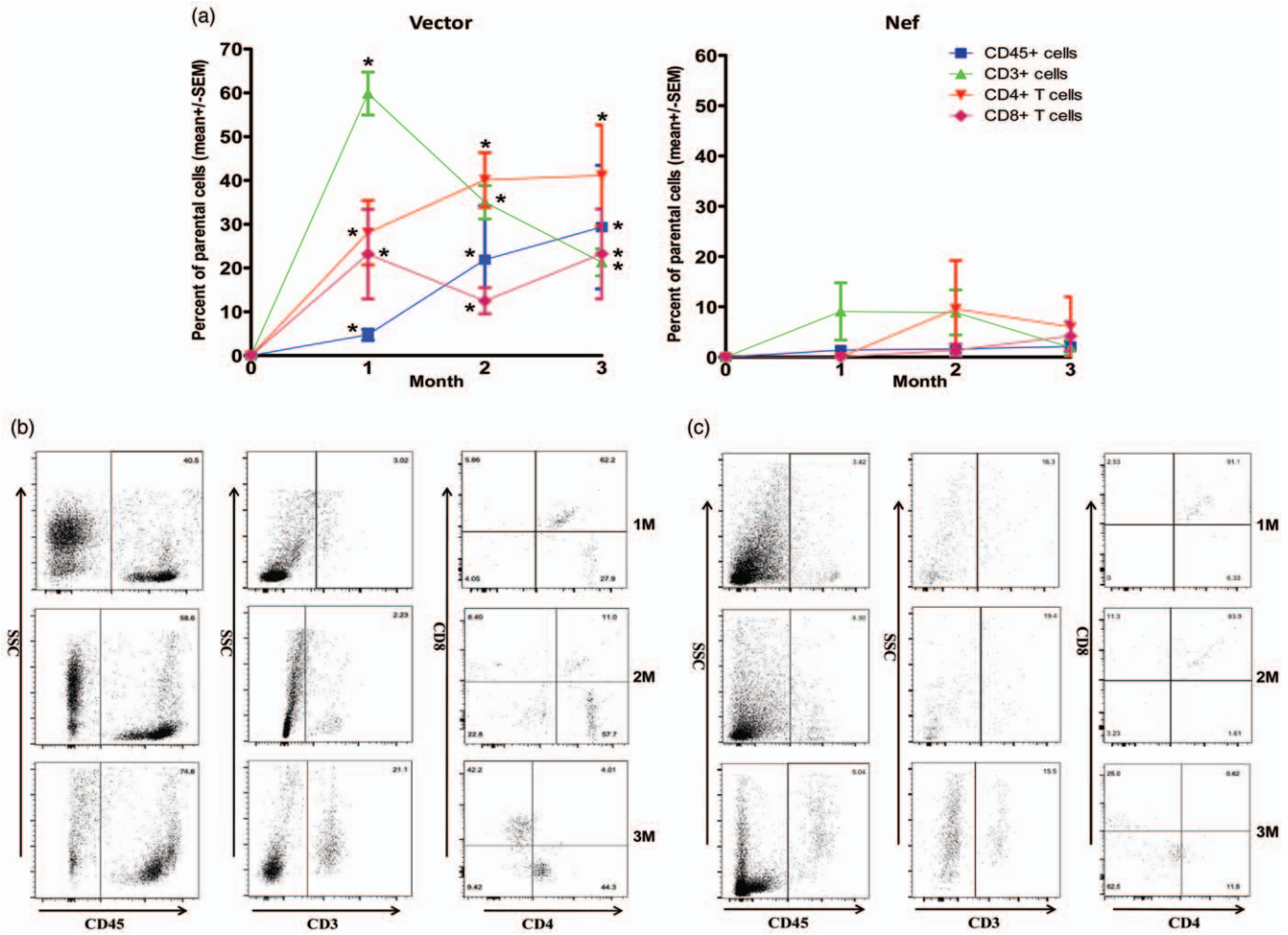

Fig. 2. Effect of Nef on the abundance of CD3+CD4$^+$ and CD3+CD8$^+$ T cells in the peripheral blood of humanized mice. LVX-vector or LVX-nef transduced CD34+ cells were transplanted into radiograph irradiated NCG mice. The presence of human CD3+CD4$^+$ and CD3+CD8$^+$ T cells in the peripheral blood of these mice was monitored every month for 3 months. The cumulative flow data of three bleedings of all mice in each group are shown in (a), and representative flow images of each bleeding from mice in both groups are shown in (b) (vector) and (c) (Nef) ($n = 5$ for vector group and $n = 7$ for nef group). $^*P < 0.05$.

of mice were examined for Nef expression by immunohistochemistry, and Nef was detected in all mice of the Nef group but not in the control mice (Supplemental Fig. 3, http://links.lww.com/QAD/C16). These results indicate Nef was expressed in the HSPCs and the transplanted humanized mice.

Nef altered gene expression patterns of CD34+CD38− hematopoietic stem/progenitor cells

To understand the mechanisms of action of Nef, approximately 500 *nef*-expressing HSPCs from two different donors with two technical replicates each were prepared for Smart-SeqII RNA-sequencing. The overall gene expression values of the transcriptome of all samples were compared, and multi-dimensional scaling plots of all samples were made (Supplemental Fig. 4, http://links.lww.com/QAD/C17 and Fig. 5, http://links.lww.com/QAD/C18). In total, 176 differentially expressed genes were found (Fig. 5a). Gene ontology analysis demonstrated these genes were involved mainly in leukocyte migration and chemotaxis (Fig. 5b). KEGG enrichment analysis showed these differentially expressed genes were enriched in functions related to chemokine, TLR, tumor necrosis factor, and NOD-like receptor signaling (Fig. 5c). In addition, 31 genes were found involved in the pathways of cellular senescence, pyroptosis, necroptosis, and necrosis, and necrosis seemed to be the most prominent pathway in inducing the death of HSPCs (Supplemental Table 1, http://links.lww.com/QAD/C10). A complete list of the 176 differentially expressed genes (http://links.lww.com/QAD/C11) and the genes enriched in gene ontology (http://links.lww.com/QAD/C12) and KEGG analyses (http://links.lww.com/QAD/C13) are in Supplemental data. By constructing the interaction network of proteins

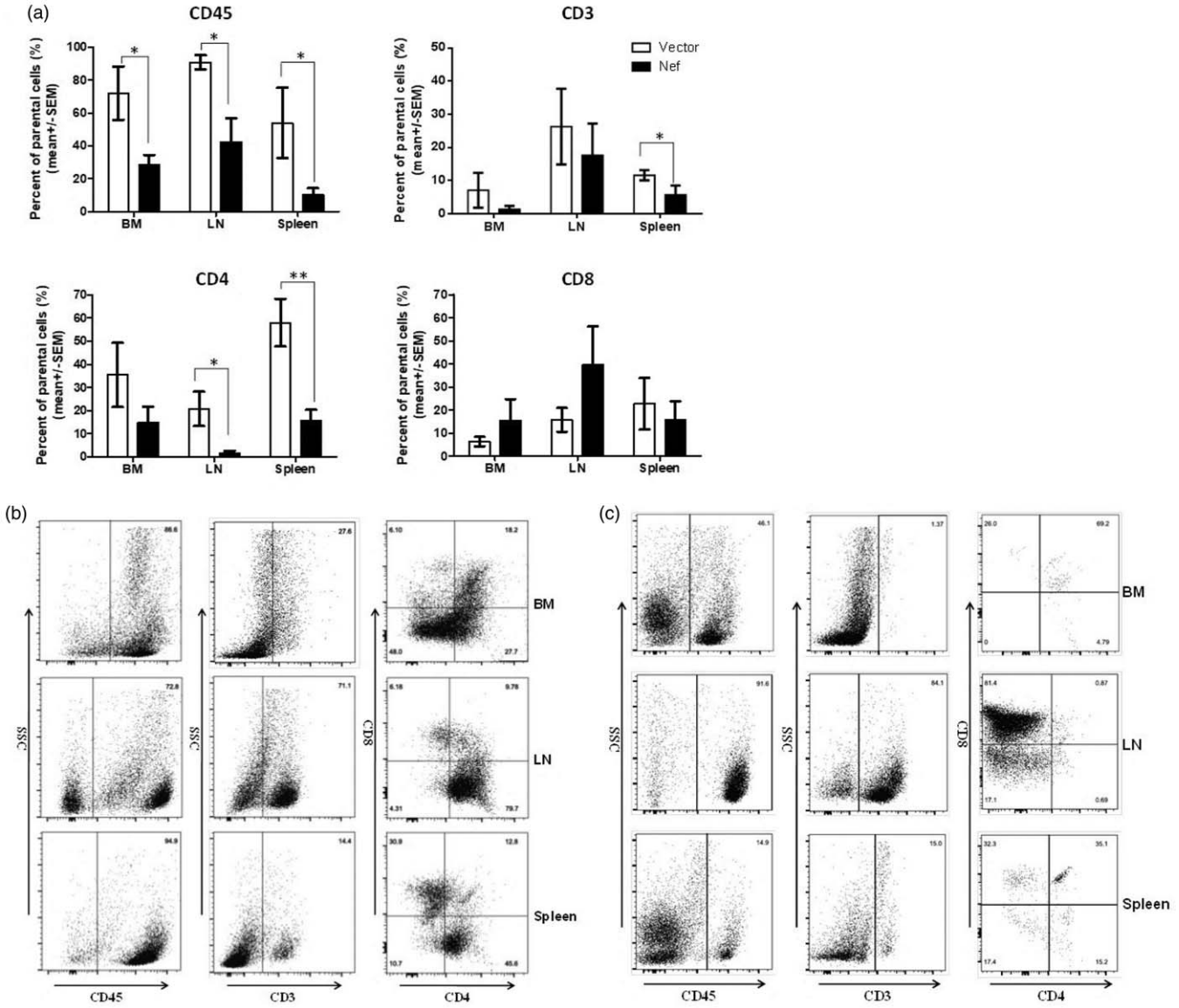

Fig. 3. Effect of Nef on the abundance of CD45+, CD3+, CD4$^+$, and CD8$^+$ cells in lymph nodes, spleens, and bone marrow of humanized mice by flow analysis. LVX-vector or LVX-nef transduced CD34+ cells were transplanted into radiograph irradiated immune deficient mice. Three months after transplantation, mice were sacrificed, and mononuclear cells were isolated from lymph nodes, spleen, and bone marrow. These cells were then stained for CD45/CD3/CD4$^+$/CD8$^+$ for flow analysis. Representative flow images are shown in (b) (vector) and (c) (nef), and the cumulative flow data of cells from each organ of all mice in each group are shown in (a) ($n = 5$ for vector group and $n = 7$ for nef group). $^*P < 0.05$; $^{**}P < 0.01$.

encoded by the differentially expressed genes, we found 111 genes involved in 307 protein–protein interactions (Fig. 5d).

Discussion

HIV-1 infection targets and most prominently causes loss of CD4$^+$ T cells. There are also negative impacts for cells not infected by the virus such as red blood cells, B cells, CD8$^+$ T cells, and natural killer cells. Thus, it is possible that HIV-1 impacts CD4$^+$ T cells not only by killing mature cells but also by disrupting the functioning of HSPCs and stromal cells in the bone marrow [28] thus affecting the development and production of mature CD4$^+$ T cells. Indeed, it has long been known that HIV-1 inhibited multi-lineage hematopoiesis in the SCID-hu (Thy/liv) mouse model [29]. In this model, HIV-1 not only caused severe depletion of human thymocytes but also severely decreased the ex-vivo recovery of human progenitor cells capable of differentiation into both erythroid and myeloid lineage cells [29]. This phenomenon was more prominent for the highly pathogenic X4-

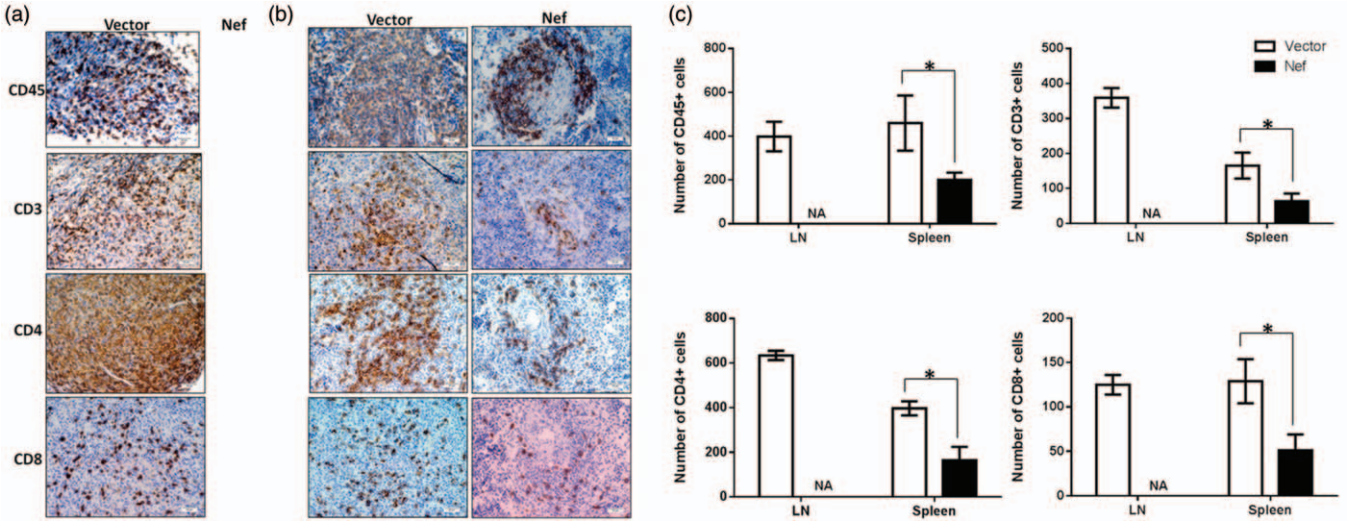

Fig. 4. Effect of Nef on the abundance of CD45+, CD3+, CD4$^+$, and CD8$^+$ cells in the lymph nodes and spleens of humanized mice by immunohistochemistry (IHC) staining. Lymph nodes and spleens from humanized mice were also examined by IHC for CD45+, CD3+, CD4$^+$, and CD8$^+$ cells. No lymph nodes in the Nef group were harvested for IHC due to limited number. Representative staining images are shown in (a) (lymph nodes) and (b) (spleen), and the cumulative data of positive cells from mice in each group are shown in (c) ($n = 5$ for vector group and $n = 7$ for nef group). NA, not available. $^*P < 0.05$.

tropic viruses. This study also found abnormal hematopoiesis was present in the SCID-hu mice even when viral suppression was achieved with antiretroviral therapy [29] suggesting there were factors independent of viral replication *per se* that contribute to the observed hematopoietic abnormalities [1]. In addition, it is important to note during the course of the infection CD34+ cells were not lost from the thymic organoid. Consistent with above observations, Sauce *et al.* [1] found the level of CD34+ cells circulating in blood of HIV-1-infected individuals was maintained regardless of the severity of the disease course.

Our previous work revealed reduced thymic T-cell output contributed to CD4$^+$ T-cell depletion in the humanized mice infected with HIV-1_{LAI} and this reduction was not directly associated with viral replication [8,9]. In other words, thymocyte loss was greatly prevented in HIV-1_{LAI} infection where *nef* was deleted despite a high viral load [8,9]. In the current study, we further investigated whether HIV-1_{LAI} Nef affected the development of T lymphoid cells from HSPCs with a non-infection experimental design that is distinct from the damage inflicted by the infection process *per se*. Our results showed *nef* expression in HSPCs blocked their development into T lymphoid cells both *in vitro* and in the mice reconstituted with *nef*-expressing HSPCs. This block could contribute to reduced levels of circulating CD45+ cells and those present in the tissues of the mice seeded with *nef*-expressing CD34+ cells. In the context of an overall loss of CD45+ cells, we observed a significant loss of CD4$^+$ T cells in lymph nodes but not of CD8$^+$ T cells. The lack of other viral proteins in our system allows for straightforward attribution of hematopoietic defects to Nef.

It is reported that HIV-1 and SIV Nef inhibited the differentiation of macaque HSPCs into multiple lineages of hematopoietic cells by affecting the NEF/PPARγ/STAT5 signaling pathway [13]. Significantly, these effects were not seen with pathogenically weaker HIV-2 suggesting that Nef dependent hematopoietic defects during HIV-1 infection could contribute to overall pathogenesis [30]. Based on the results in current study and our previous study, we speculate the point where Nef blocks hematopoiesis is at the level of HSPC differentiation into distinct hematopoietic lineages [31]. This conclusion is supported by our finding that *nef*-expressing CD34+ cells were not lost and other previous studies [1,29]. Our RNA-seq of *nef*-expressing CD34+CD38− cells revealed the expression of 176 genes was altered by Nef. However, the detailed mechanisms how the alteration of these genes by Nef affects HSPC development remain to be investigated.

In this study, our overall results suggest the initial impact of Nef may be inducing cell death of HSPCs but significant numbers of cells escape and subsequently encounter additional sites of differentiation inhibition, which eventually leads to the failure of T-cell development in our system. Alternatively, death of mature T lymphocytes, especially CD4$^+$ T lymphocytes, is possible to be an another mechanism of T-cell loss due to *nef* expression in our study considering that a recent study demonstrated that *nef* expression was necessary for systemic and substantial CD4$^+$ T-cell loss in HIV-1 infection [32]. Further studies are needed to understand the interaction of Nef with the 176 genes identified in our study, and therapeutics targeting Nef could potentially correct hematopoietic abnormalities in HIV-1-infected individuals.

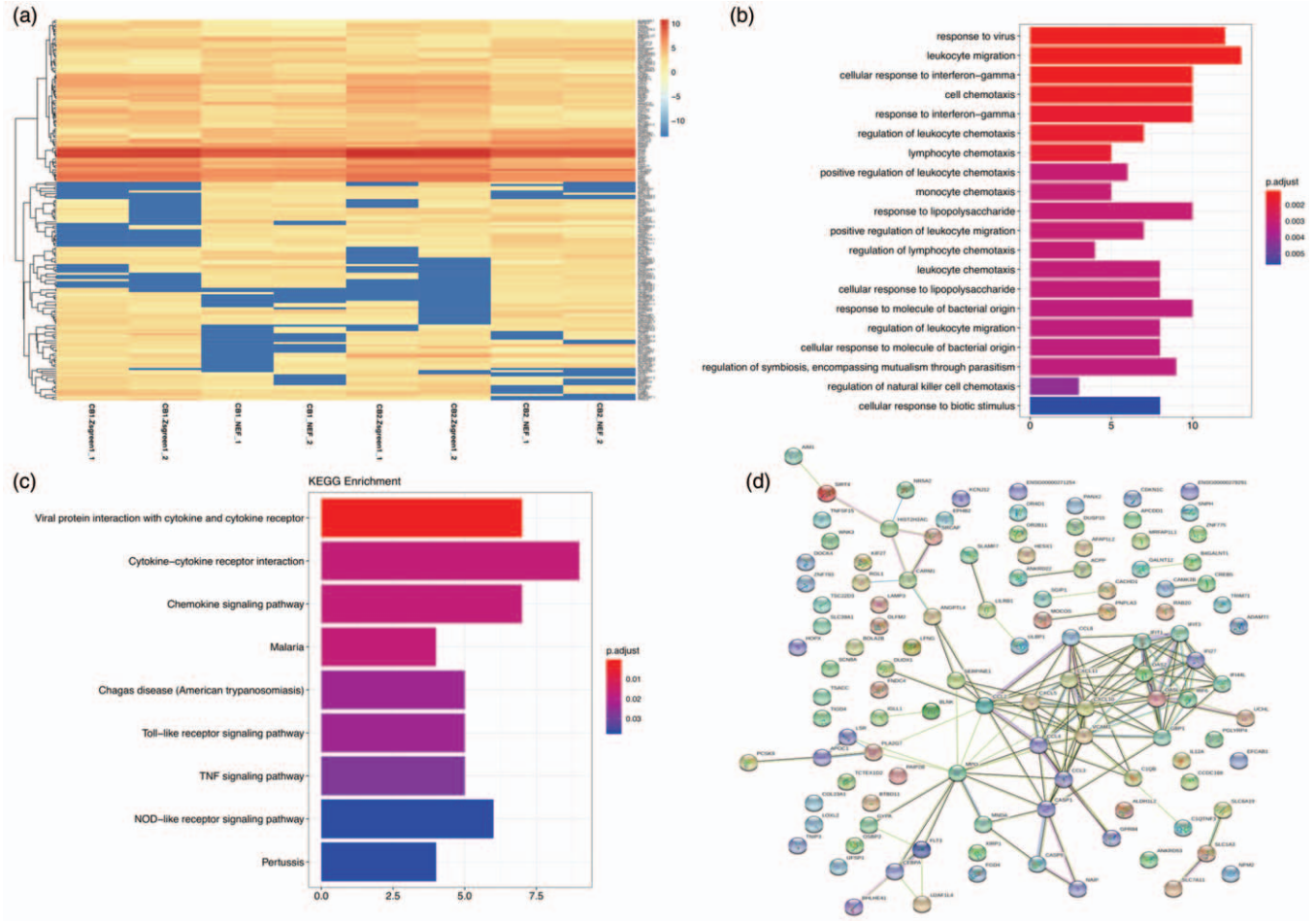

Fig. 5. Effect of Nef on gene expression in CD34+CD38− hematopoietic stem/progenitor cells. Flow cytometry-enriched CD34+CD38−Zsgreen1+ cells with or without *nef* expression were subjected to Smart-seqII RNA-seq. The heatmap of differentially expressed genes is shown in (a). The log values of expression levels of various genes are shown with different colors. Results of gene ontology analysis of differentially expressed genes are shown in (b). Results of Kyoto Encyclopedia of Genes and Genomes analysis of differentially expressed genes are shown in (c). Box length indicates the number of differentially expressed genes in each pathway. The protein–protein interaction network of proteins encoded by differentially expressed genes is shown in (d).

Acknowledgements

Tongjie Wang and Chengxiang Xia from the CAS Key Laboratory of Regenerative Biology, Guangzhou Institutes of Biomedicine and Health, Chinese Academy of Sciences did the Smart-seqII sequencing and analyzed the sequencing data. Here we acknowledge their contribution to this work.

Authors' contributions: W.Z. designed the study, performed the experiments, and wrote the article; J.X., F.W., X.C., Q.L., J.W., S.Z., L.C., X.F., Z.Z., and Z.W. performed the experiments; J.X. collected all the flow data; F.W., X.C., Q.L. collected cord blood samples; J.W. and S.Z. did the co-culture experiments; L.C. did all the flow sorting experiments; X.F., Z.Z., and Z.W. did the IHC, WB, and mouse work. All authors read and approved the final article.

This work was supported by the National Natural Science Foundation of China (grant nos.: 81660279 and 81701629), Jiangxi Department of Science and Technology (grant nos.: 20161ACB21016, 20171BCB23088, 20181ACH80002, and 20202BAB206023), and the startup funding for scholars returned from abroad from the Ministry of Education, P.R.C. (grant no.: 2015060020102070).

Conflicts of interest

The authors declare that they have no conflicts of interests.

References

1. Sauce D, Larsen M, Fastenackels S, Pauchard M, Ait-Mohand H, Schneider L, *et al*. **HIV disease progression despite suppression of viral replication is associated with exhaustion of lymphopoiesis.** *Blood* 2011; **117**:5142–5151.

2. Ferrando-Martinez S, De Pablo-Bernal RS, De Luna-Romero M, De Ory SJ, Genebat M, Pacheco YM, *et al*. **Thymic function failure is associated with human immunodeficiency virus disease progression.** *Clin Infect Dis* 2017; **64**:1191–1197.
3. Maciejewski JP, Weichold FF, Young NS. **HIV-1 suppression of hematopoiesis in vitro mediated by envelope glycoprotein and TNF-alpha.** *J Immunol* 1994; **153**:4303–4310.
4. Calenda V, Graber P, Delamarter JF, Chermann JC. **Involvement of HIV nef protein in abnormal hematopoiesis in AIDS: in vitro study on bone marrow progenitor cells.** *Eur J Haematol* 1994; **52**:103–107.
5. Moses A, Nelson J, Bagby GC Jr. **The influence of human immunodeficiency virus-1 on hematopoiesis.** *Blood* 1998; **91**:1479–1495.
6. Davinelli S, Scapagnini G, Denaro F, Calabrese V, Benedetti F, Krishnan S, *et al*. **Altered expression pattern of Nrf2/HO-1 axis during accelerated-senescence in HIV-1 transgenic rat.** *Biogerontology* 2014; **15**:449–461.
7. Brothers TD, Rockwood K. **Biologic aging, frailty, and age-related disease in chronic HIV infection.** *Curr Opin HIV AIDS* 2014; **9**:412–418.
8. Watkins RL, Zou W, Denton PW, Krisko JF, Foster JL, Garcia JV. **In vivo analysis of highly conserved Nef activities in HIV-1 replication and pathogenesis.** *Retrovirology* 2013; **10**:125.
9. Zou W, Denton PW, Watkins RL, Krisko JF, Nochi T, Foster JL, *et al*. **Nef functions in BLT mice to enhance HIV-1 replication and deplete CD4+CD8+ thymocytes.** *Retrovirology* 2012; **9**:44.
10. McNamara LA, Onafuwa-Nuga A, Sebastian NT, Riddell J, Bixby D, Collins KL. **CD133+ hematopoietic progenitor cells harbor HIV genomes in a subset of optimally treated people with long-term viral suppression.** *J Infect Dis* 2013; **207**:1807–1816.
11. Buzon MJ, Sun H, Li C, Shaw A, Seiss K, Ouyang Z, *et al*. **HIV-1 persistence in CD4+ T cells with stem cell-like properties.** *Nat Med* 2014; **20**:139–142.
12. Zhang J, Crumpacker C. **Hematopoietic stem and immune cells in chronic HIV infection.** *Stem Cells Int* 2015; **2015**:148064.
13. Prost S, Le Dantec M, Auge S, Le Grand R, Derdouch S, Auregan G, *et al*. **Human and simian immunodeficiency viruses deregulate early hematopoiesis through a Nef/PPARgamma/STAT5 signaling pathway in macaques.** *J Clin Invest* 2008; **118**:1765–1775.
14. Ye Z, Yu X, Cheng L. **Lentiviral gene transduction of mouse and human stem cells.** *Methods Mol Biol* 2008; **430**:243–253.
15. Mazumdar C, Shen Y, Xavy S, Zhao F, Reinisch A, Li R, *et al*. **Leukemia-associated cohesin mutants dominantly enforce stem cell programs and impair human hematopoietic progenitor differentiation.** *Cell Stem Cell* 2015; **17**:675–688.
16. Li M, Liu F, Zhang F, Zhou W, Jiang X, Yang Y, *et al*. **Genomic ERBB2/ERBB3 mutations promote PD-L1-mediated immune escape in gallbladder cancer: a whole-exome sequencing analysis.** *Gut* 2019; **68**:1024–1033.
17. Cao Z, Ye T, Sun Y, Ji G, Shido K, Chen Y, *et al*. **Targeting the vascular and perivascular niches as a regenerative therapy for lung and liver fibrosis.** *Sci Transl Med* 2017; **9**:eaai8710.
18. Trapnell C, Roberts A, Goff L, Pertea G, Kim D, Kelley DR, *et al*. **Differential gene and transcript expression analysis of RNA-seq experiments with TopHat and Cufflinks.** *Nat Protoc* 2012; **7**:562–578.
19. Love MI, Huber W, Anders S. **Moderated estimation of fold change and dispersion for RNA-seq data with DESeq2.** *Genome Biol* 2014; **15**:550.
20. Subramanian A, Tamayo P, Mootha VK, Mukherjee S, Ebert BL, Gillette MA, *et al*. **Gene set enrichment analysis: a knowledge-based approach for interpreting genome-wide expression profiles.** *Proc Natl Acad Sci U S A* 2005; **102**:15545–15550.
21. Yu G, Wang LG, Han Y, He QY. **clusterProfiler: an R package for comparing biological themes among gene clusters.** *OMICS* 2012; **16**:284–287.
22. Crompton T, Outram SV, Hager-Theodorides AL. **Sonic hedgehog signalling in T-cell development and activation.** *Nat Rev Immunol* 2007; **7**:726–735.
23. Dik WA, Pike-Overzet K, Weerkamp F, de Ridder D, de Haas EF, Baert MR, *et al*. **New insights on human T cell development by quantitative T cell receptor gene rearrangement studies and gene expression profiling.** *J Exp Med* 2005; **201**:1715–1723.
24. Van Coppernolle S, Verstichel G, Timmermans F, Velghe I, Vermijlen D, De Smedt M, *et al*. **Functionally mature CD4 and CD8 TCRalphabeta cells are generated in OP9-DL1 cultures from human CD34+ hematopoietic cells.** *J Immunol* 2009; **183**:4859–4870.
25. Timmermans F, Velghe I, Vanwalleghem L, De Smedt M, Van Coppernolle S, Taghon T, *et al*. **Generation of T cells from human embryonic stem cell-derived hematopoietic zones.** *J Immunol* 2009; **182**:6879–6888.
26. Sebastian NT, Zaikos TD, Terry V, Taschuk F, McNamara LA, Onafuwa-Nuga A, *et al*. **CD4 is expressed on a heterogeneous subset of hematopoietic progenitors, which persistently harbor CXCR4 and CCR5-tropic HIV proviral genomes in vivo.** *PLoS Pathog* 2017; **13**:e1006509.
27. Lamas-Murua M, Stolp B, Kaw S, Thoma J, Tsopoulidis N, Trautz B, *et al*. **HIV-1 Nef disrupts CD4 (+) T lymphocyte polarity, extravasation, and homing to lymph nodes via its Nef-associated kinase complex interface.** *J Immunol* 2018; **201**:2731–2743.
28. Yuan YH, Zhao SS, Wang XL, Teng ZP, Li DS, Zeng Y. **HIV-1 p55-gag protein induces senescence of human bone marrow mesenchymal stem cells and reduces their capacity to support expansion of hematopoietic stem cells in vitro.** *Cell Biol Int* 2017; **41**:969–981.
29. Koka PS, Fraser JK, Bryson Y, Bristol GC, Aldrovandi GM, Daar ES, *et al*. **Human immunodeficiency virus inhibits multilineage hematopoiesis in vivo.** *J Virol* 1998; **72**:5121–5127.
30. Gautier D, Beq S, Cortesao CS, Sousa AE, Cheynier R. **Efficient thymopoiesis contributes to the maintenance of peripheral CD4 T cells during chronic human immunodeficiency virus type 2 infection.** *J Virol* 2007; **81**:12685–12688.
31. Laurenti E, Gottgens B. **From haematopoietic stem cells to complex differentiation landscapes.** *Nature* 2018; **553**:418–426.
32. Furler RL, Ali A, Yang OO, Nixon DF. **Nef-induced differential gene expression in primary CD4+ T cells following infection with HIV-1 isolates.** *Virus Genes* 2019; **55**:541–544.